IEEE Access
Multidisciplinary | Rapid Review | Open Access Journal

Received June 20, 2021, accepted July 17, 2021, date of publication July 26, 2021, date of current version August 3, 2021.

Digital Object Identifier 10.1109/ACCESS.2021.3099109

Improved Flux Tracing Method Based on Parametric Curve for Calculating Ion Flow Field of HVDC Transmission Lines

JIN-HYEOK KIM[1], SUNGJUNG JOO[1], AND YOUNG-SEEK CHUNG[2], (Member, IEEE)
[1]Korea Research Institute of Standards and Science, Daejeon 34113, South Korea
[2]Department of Electronic Convergence Engineering, Kwangwoon University, Seoul 01897, South Korea

Corresponding author: Young-Seek Chung (yschung@kw.ac.kr)

This work was supported by the Research on Development of Physical Standards for Measurement through the Korea Research Institute of Standards and Science under Grant KRISS-2021-GP2021-0002.

ABSTRACT An improved method for tracing electric flux lines in the vicinity of the overhead high voltage direct current (HVDC) transmission lines is developed by using parametric curves. Based on the geometric relation between the electric field vector and the derivative of the parametric curve function, the electric flux lines can be successfully traced without accumulation of the numerical error caused by the differentiation for calculating the electric potential. Considering the structural characteristics of the transmission line, the control points at both ends of the parametric curve can be easily located, and the remaining control points are modified to minimize an error function defined by the electric field vectors at nodes along the curve. Once the electric flux lines are traced, a series of flux tubes is created by bundling adjacent flux lines, and the nodal electric field vectors and space charge densities are iteratively updated. In order to consider the ionized space charge effect, new flux lines of modified electric field are traced, which in turn affects the existing space charge distribution. The process is repeated until the effect of the space charge is fully considered. The performance of the proposed algorithm is verified by comparing the resulting ground profiles of the ion flow field distribution with the result of the analytical model and the long-term measurement of the full-scale transmission line.

INDEX TERMS Corona discharge, flux tracing method, HVDC transmission, ion flow field, space charge.

I. INTRODUCTION

The ionized space charges generated by corona discharge on the surface of the overhead high voltage direct current (HVDC) transmission conductors flow into inter-electrode space under the effect of various types of forces. In general, the ion trajectories are mainly influenced by three factors: 1) the electric field distribution determined by the voltage applied to the conductor and the ionic polarity, 2) the electrostatic force between ionized space charges, and 3) mechanical force exerted by wind of atmospheric air. The factors listed above will determine the transport direction of the ionized space charges, and this path can be represented by a flux line starting from the discharging surface to ground (or the surface to conductors with the opposite polarity). Unlike the AC transmission environment, the static electric field distribution produced by the DC conductor causes the ion trajectory to be directed in a constant direction resulting in a power loss due to the continuous current flow drain from the source [1].

Since the first approach to obtain an analytical solution for a concentric cylindrical configuration was developed by Townsend [2] in the early 1900s, attempts have been made to analyze the practical conductor-ground configuration. With several simplifying assumptions, an analytic solution for the line-to-ground configuration was proposed by Deutsch [3], and one of the assumptions in this study served as the basis for the early numerical methods. In general, the early analytic solutions were mainly focused on obtaining the voltage-current characteristic of the ion flow field in still air. As practical interest had extended to the electric field and space charge distribution in the inter-electrode region, especially on the ground plane, the first numerical method based on Deutsch's assumption were developed in 1969. Over the past half century, numerous studies have been conducted to define an appropriate numerical analysis model, which

The associate editor coordinating the review of this manuscript and approving it for publication was Ali Raza.

can be categorized into two types according to their basis: flux tracing methods and element-based methods. This article discusses the former in detail to propose an improved version of flux tracing method.

Maruvada and Janischewskyj [4], [5] developed the first numerical method based on Deutsch's assumption, which supposed that the space charge affects only the magnitude of the electric field but not its direction. In this method, an efficient evaluation of the electric field and space charge distribution was described using a computational technique, which is called the flux tracing method (FTM). The FTM introduced a field modification factor to express the electric field vector in the presence of space charge. Based on Deutsch's assumption, the electric field and space charge distributions can be described with respect to the variation of electric potential along the flux line. Since the flux lines specifies the transport direction of the space charges, a two-dimensional problem can be simplified into a series of one-dimensional equations and solved along each flux line.

Despite the simplicity and efficiency, a major drawback of Deutsch's assumption had been criticized by many researchers, leading to widespread use of the element-based methods. According to the experiment results conducted in [6]–[8], the result with Deutsch's assumption is acceptable when the corona discharge is either negligibly small or strong enough to be saturated. It was concluded that a distortion effect on the electric field line influenced by the ionic space charge distribution cannot be considered and that a significant amount of error could seriously affect the accuracy of calculations.

To consider a non-linearity caused by the fact that an ion flow field modifies the ionic space charge distribution while being influenced by the drifting ions, Maruvada improved the conventional FTM with an iterative scheme [9]. The repetitive evaluations and modifications of the electric field lines and space charge density could successfully describe the ionic space charge effect on the ion flow field. This iterative method was subsequently extended by the same author to consider ambient electric fields produced by atmospheric electricity at the ground surface [10] and the effect of wind velocity [11].

Several applications of FTM can be found in relatively recent literatures. Zhang *et al*. [12] used the FTM in the estimation of the initial ionic space charge distribution when developing the method of characteristics. The electric field lines around the bipolar transmission line were presented to illustrate the distortion effect by the ionic space charge distribution. An effort to combine the FTM and the finite element method (FEM) was made by the same author to reduce the calculation time of the FEM [13].

Qiao *et al*. [14] established the non-linear algebraic equations using the finite-difference method to discretize the differential equations based on the FTM. The author showed that a better convergence in the iterative process can be achieved with the directly enforce boundary condition. Based on the previous work, the author developed the iterative FTM for the AC/DC hybrid transmission lines [15].

The electric flux tracing process has also been utilized in other studies that are not based on the FTM. Abdel-Salam and Al-Hamouz [16] proposed a numerical algorithm for analyzing the unipolar ion flow field in line-to-ground transmission line configuration based on the finite-element grid and the flux tubes. The flux tubes, which is composed of the electric flux lines, are iteratively regenerated to consider the non-linearity between the electric field and space charge distribution. Recently, two different methods were presented by the same author to trace the unipolar flux lines from a starting point on the conductor surface to the ground [17]. One of the methods depends on the magnitude and direction of the electric field, and the other relies on the equation consisting of xy-coordinates and the angle of the starting point of the flux line.

A general process for tracing the electric flux lines begins with finding equipotential contours in the inter-electrode region. By definition, the direction of the electric field vector must be perpendicular to the equipotential line (or surface) at any point. Therefore, once the equipotential contours are successfully defined, the electric flux line can be traced by starting at a point on the conductor surface and continuing perpendicular to the equipotential lines until it terminates. Along the traced flux line, the current continuity equation, which is one of the governing equations, is to be solved for the electric potential and space charge density so that the current conservation law is satisfied.

In the conventional FTM, the governing equations, which consists of Poisson's equation and the current continuity equation, are solved for the scalar electric potentials instead of the electric field vectors to find the equipotential contours. Since the current continuity equation is expressed in terms of the electric field vector, which is defined as the negative gradient of a scalar potential, a numerical differentiation process is inevitable. As Takuma and Kawamoto [18] pointed out, however, first-order derivatives included in the potential term cause a significant numerical error, which is accumulated in the iteration process, resulting in divergence or oscillation of the solution. Moreover, an enforced Dirichlet boundary condition for the potentials on the outermost boundary, which is not zero in practice, can cause the backpropagation of the error within the region. In order to overcome the difficulties regarding the numerical differentiation, the numerical methods using the integral form of the current continuity equation have been proposed [19]–[22].

This article proposes a new flux tracing method based on parametric curve optimization. The flux lines are traced by minimizing an error function defined by the relation between the two vectors of the electric field and the gradient of the parametric curve. Since the derivative of the parametric curve can be analytically derived, the flux line can be traced without the numerical differentiation process by aligning two vectors at any point along the flux line. Once the flux line is successfully traced, the space charge distribution can be obtained using the integral form of the current continuity equation.

This article is organized as follows. Section I presents a historical review of published research works on the FTM and its difficulties. Section II describes the given problem with the governing equations and investigates the detailed methodology of the proposed flux tracing strategy. Section III provides the numerical results from the analytic unipolar model and the bipolar line-to-ground model to verify the effectiveness of the proposed method. Finally, Section VI presents a conclusion to review the main points of the article.

II. PROBLEM DESCRIPTION AND FORMULATION

In this section, the ion flow effect due to overvoltage induced in the overhead DC transmission line is described by the governing equations with general assumptions. In order to avoid the numerical differentiation process, a curve-based method for tracing flux lines is proposed and investigated for its physical correctness. Finally, the integral form of the current continuity equation is solved for the ionic space charge density, and the modified ion flow field line is traced iteratively to consider the non-linear interaction.

A. GOVERNING EQUATION

In general, the corona discharge resulting ionization can be mathematically defined by making several simplifying assumptions [1], and some assumptions adopted in this article are listed as follows:

1) The thickness of the ionization layer around coronating conductor is negligible compared to the distance between the conductor and ground plane.
2) The electric field remains constant at the corona onset gradient of the conductor.
3) The constants for ionic mobility depends on the ionic polarity and assumed to be independent of the electric field strength.
4) The wind velocity is assumed to be time-invariant.

By the first assumption, the inter-electrode region is assumed to be filled with the ionic space charges. The second assumption simplifies the complex ionization process on the discharging surface in terms of the magnitude of the electric field [23]. This assumption is used as a forced boundary condition at the surface of the conductor. The third and fourth assumptions simplify the expression of the ion current density in the current continuity equation.

The non-linear relation between the electric field and ionic space charge distribution can be described by the following equations [1].

$$\nabla \cdot \mathbf{E} = \frac{(\rho_+ - \rho_-)}{\varepsilon_0} \tag{1}$$

$$\mathbf{J}_\pm = \rho_\pm \left\{ \mu_\pm \mathbf{E} \mp \left(\frac{D_\pm}{\rho_\pm} \nabla \rho_\pm \right) \pm \mathbf{W} \right\} \tag{2}$$

$$\nabla \cdot \mathbf{J}_\pm = \mp \frac{R_i \rho_+ \rho_-}{e} \tag{3}$$

where $\mathbf{E}$ and, $\mathbf{J}$ are the electric field and the current density vectors at any point in space, respectively, ρ is the ionic space charge density, ε_0 is the permittivity of free space, μ is the ionic mobility, D is the diffusion coefficients of ions, $\mathbf{W}$ is the time-invariant wind velocity vector, R_i is the recombination coefficient, and e the electron charge. The signs on μ, ρ, and $\mathbf{J}$ are the polarities of the ionic mobility, charge density, and resulting current density, respectively.

The space charge distribution is influenced by the electric field produced by the induced voltage on the conductor, and the modified ionic space charge distribution affects the existing electric field in space. In the iterative scheme, both $\mathbf{E}$ and ρ are updated to satisfy (1) to (3). In this article, as in other integral-based methods, (1) is discarded, and the integral form of (3) will be presented in Section II-C.

B. FLUX LINES BASED ON PARAMETRIC CURVE

A Bezier curve is a space curve, which is contained within the convex hull of the Bezier polygon defined by several control points. Due to the fact that the tangent vectors at each end are directed along the first and last span of the polygon, boundary conditions for the electric field on the conductor surface and ground plane can be easily satisfied. Also, since the electric field distribution is continuous and smooth in the inter-electrode region, the flux lines can be represented by parametric curves that are assumed to originate from the conductor surface and terminate on the ground plane or the other conducting surfaces with the opposite polarity. The shape of the curve can be determined by adjusting the locations of several control points. The physical correctness and effectiveness of the curve-based approach will be discussed in this section.

A parametric Bezier curve of degree M is defined as

$$\mathbf{B}(\tau) = \sum_{i=0}^{M} {}^{M}C_i \mathbf{P}_i (1-\tau)^{M-i} \tau^i \tag{4}$$

where τ is parameters defined from 0 to 1, i the summation index, C the binomial coefficient, and $\mathbf{P}_i$ the i^{th} control point out of M points. In the unipolar conductor-plane configuration, the first point $\mathbf{P}_0$ and the last point $\mathbf{P}_M$ are subject to be located on the conductor surface and on the ground, respectively. Note that $\mathbf{B}$ does not stand for the magnetic field intensity, which is not considered in this article. A Bezier curve of degree 3 is shown in Fig. 1(a) for example. In this case, P_0 and P_3 are fixed at the conductor surface and the ground plane, respectively, while the rest of control points are adjusted to determine the shape of the curve.

The derivative of (4) with respect to τ is well-known and can be expressed as

$$\mathbf{B}'(\tau) = \sum_{i=0}^{M-1} M (\mathbf{P}_{i+1} - \mathbf{P}_i) b_{M-1,i} \tag{5}$$

where $b_{M,i}$ is Bernstein basis polynomials of degree M and is equal to ${}^{M}C_i(1-\tau)^{M-i}\tau^i$. Since $\mathbf{B}$ is supposed to be shaped after the electric flux line, $\mathbf{B}'$ must be tangential to the electric field vectors at any point along the curve. In addition, $\mathbf{B}'(0)$ and $\mathbf{B}'(1)$ must be normal to the conductor surface and ground plane, respectively.

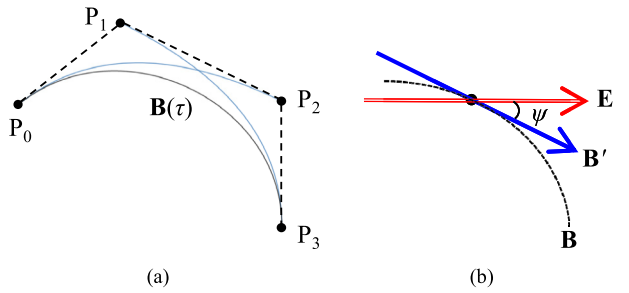

FIGURE 1. An example of parametric curve. (a) A Bezier curve of degree 3. (b) The relative angle difference between E and B′.

Based on the derivatives and electric field vectors along the curve, an error function can be defined as follows.

$$\varepsilon = \frac{1}{2}(1 - \cos\psi)^2 \tag{6}$$

where $\cos\psi = (\mathbf{E}\cdot\mathbf{B}')/(|\mathbf{E}|\,|\mathbf{B}'|)$ from the relative angle difference ψ between $\mathbf{E}$ and $\mathbf{B}'$ as shown in Fig. 1(b).

The error function above represents the difference in directions between the tangential components of the curve and electric field vectors at any point along the flux line. Therefore, an electric flux line can be successfully traced with the adjusted control points by minimizing the error defined in (6).

To minimize the error function, various techniques such as the least square method (LSM), the pattern search method (PSM), and the steepest descent method (SDM) can be utilized. In this article, in order to deal with the non-linear relation between the coordinates of $\mathbf{P}_M$ on the arbitrary shaped boundary, the SDM-based optimization algorithm is used to determine the control points.

In the SDM-based algorithm, the local minima for any given function can be searched by utilizing the steepest gradient in an iterative manner. The gradient of the error function with respect to the control points is used to determine the direction of fastest decrease toward the minimum, and the searching process is controlled by a relaxation factor. The updated control points to minimize (6) can be obtained as

$$\mathbf{P}^{k+1} = \mathbf{P}^k - \gamma\frac{\nabla\varepsilon^k}{|\nabla\varepsilon^k|^2}\cdot\varepsilon^k \tag{7}$$

where k represents the iteration number, and γ is the relaxation factor which is generally less than or equal to unity.

The gradient of the error function in (7) with respect to the control point can be derived as

$$\frac{\partial\varepsilon}{\partial P_i} = -\left(1-\cos\psi_{p_i}\right)\cdot\frac{\partial\cos\psi_{p_i}}{\partial P_i} \tag{8}$$

$$\frac{\partial\cos\psi_{p_i}}{\partial P_i} = \frac{\mathbf{E}_{p_i}}{|\mathbf{E}_{p_i}|}\cdot\left[\frac{1}{|\mathbf{B}'_{p_i}|^2}\left(-\frac{\partial|\mathbf{B}'_{p_i}|}{\partial P_i}\mathbf{B}'_{p_i} + |\mathbf{B}'_{p_i}|\frac{\partial\mathbf{B}'_{p_i}}{\partial P_i}\right)\right] \tag{9}$$

where the subscript P_i indicates the i^{th} control point at which the error is defined by (6).

Substituting (5) into (9) and simplifying with a parametric function K, the gradient of the error function at a specific control point $P_i(x_i, y_i)$ can be expressed as

$$\frac{\partial\varepsilon}{\partial x_i} = (1-\cos\psi_i)\frac{K'_i}{|\mathbf{B}'_i|^2}\left(\mathbf{B}'_{x_i}\cos\psi_i - \frac{|\mathbf{B}'_i|}{|\mathbf{E}_i|}E_{x_i}\right) \tag{10}$$

$$\frac{\partial\varepsilon}{\partial y_i} = (1-\cos\psi_i)\frac{K'_i}{|\mathbf{B}'_i|^2}\left(\mathbf{B}'_{y_i}\cos\psi_i - \frac{|\mathbf{B}'_i|}{|\mathbf{E}_i|}E_{y_i}\right) \tag{11}$$

$$K'_i = \tau^i(1-\tau)^{M-i}\left(\frac{i}{\tau} + \frac{M-i}{1-\tau}\right) \tag{12}$$

The space-charge-free electric field used in (6) can be evaluated at any point in space from the surface charge density generated by the conductor voltage. The unknown surface charge density can be calculated by the method of moment (MoM). The computational load can be significantly reduced by concentrating the region of interest on the conductor surface where the charge can actually exist. A detailed MoM formulation is presented in [22].

The process for tracing the flux line can be described by the following steps.

- Step 1) An initial flux line is assumed by (4) with $\mathbf{P}_0$ fixed at a specific point on the conductor surface and $\mathbf{P}_M$ located on the ground plane. $\mathbf{P}_1$ and $\mathbf{P}_{M-1}$ are set to satisfy the boundary conditions on the conductor surface and ground plane.
- Step 2) The derivative of the curve is calculated by (5).
- Step 3) The error function is defined along the curve by (6).
- Step 4) The coordinates of control points are modified to minimize the error function.
- Step 5) The flux line is traced and represented by the Bezier curve with new control points modified in Step 4).

The preceding five steps are repeated for different points around the conductor surface to obtain the entire flux lines in the region of interest. The overall procedure of the proposed algorithm is shown in Fig. 2.

For a unipolar DC line conductor 0.1 m in radius suspended 2 m above a ground plane, the flux lines for the electrostatic field are shown in Fig. 3. Gray dotted lines are the initial curve assumed in Step 1), and solid lines are the final Bezier curve. In this case of the unipolar configuration, only y-coordinates of the last control points are restrained to be zero to ensure that they are properly grounded. Fig. 4 shows the error defined by (6), which is normalized as a ratio to the initial value. The normalized amount of error is reduced to less than 1% of the initial error after 20 iterations, and it converged to the order of 10^{-5}% of the initial value.

The proposed method is applicable to the bipolar line-to-ground configuration. In this case, the flux lines can be terminated either the ground plane or the surface of the conductor with the opposite polarity. In terms of the physical characteristic of the electric field distribution between the conductors of two different polarities, however, a single curve may not

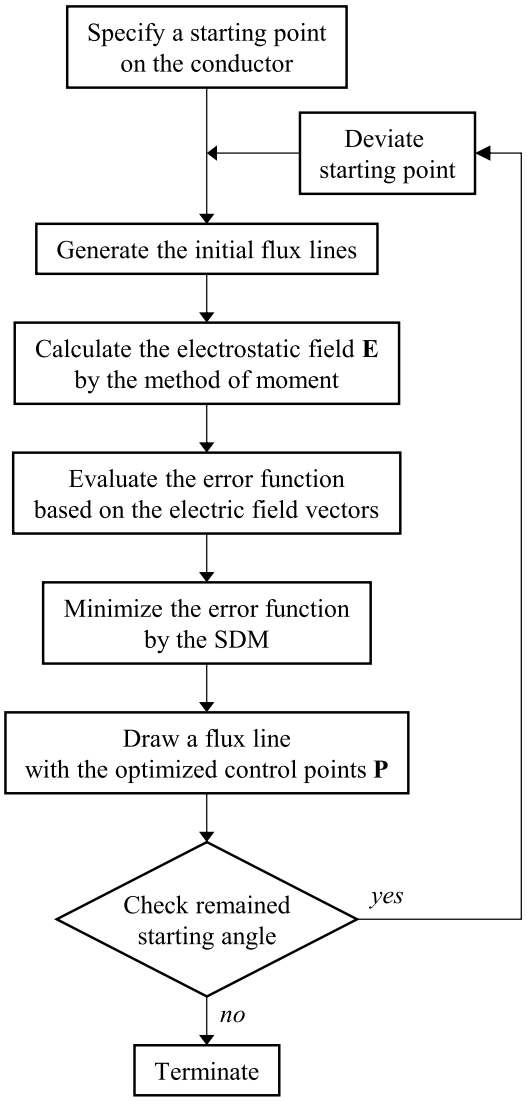

FIGURE 2. Flowchart of the proposed flux tracing algorithm.

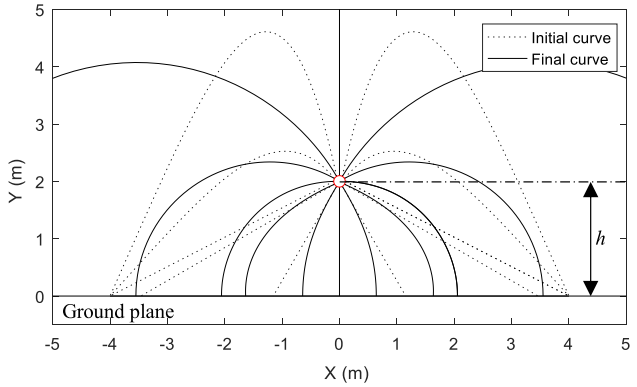

FIGURE 3. Traced flux lines around a unipolar DC transmission line based on Bezier curve optimization.

be sensitive enough to represent the flux line. In addition, the distorted flux line by the ionic space charge may not be assumed to be smooth anymore. Therefore, a piecewise technique must be introduced to trace an arbitrarily shaped flux line.

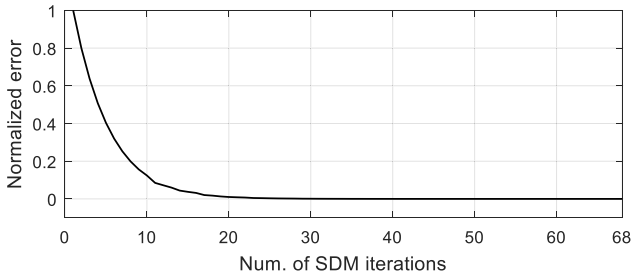

FIGURE 4. Amount of error through the SDM iteration normalized to the initial value.

The piecewise Bezier curve optimization algorithm provides an ability to trace the flux lines, which are assumed to be distorted by the physical factors such as the line polarity, the ionic space charge distribution, and the wind velocity. In the piecewise algorithm, a set of Bezier curves is used to trace a single flux line. The x-domain is divided into m subdomains, the length of which depends on the instantaneous rate of change of the flux line. The starting point of the first curve remains at the conductor surface, but the last control point is assumed to be located at the end of the first subdomain. Once the curve is optimized in the first subdomain, the second curve starts at the end point of the first curve while maintaining its slope. This process is repeated for the entire subdomain until the curve reaches the outmost boundary. The electric flux lines for the bipolar line configuration is presented in Fig. 5. It shows that the abrupt changes in the electric field distribution, especially near the origin, are traceable by the piecewise Bezier curve optimization.

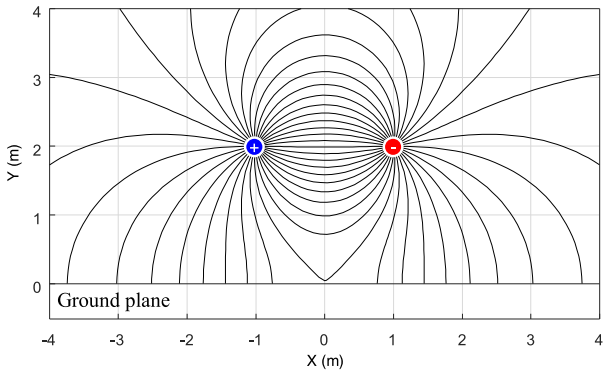

FIGURE 5. Traced flux lines for the bipolar line configuration using the piecewise Bezier curve optimization.

The presence of wind in the transverse direction to the transmission line will also influence the ion trajectories. As stated in [11], the current density in (2) can be reorganized to combine the effects of the electric field and wind velocity as

$$\mathbf{J}_{\pm} = \mu_{\pm}\rho_{\pm}\left(\mathbf{E} + \frac{\mathbf{W}}{\mu_{\pm}}\right). \tag{13}$$

In this case, the effect of ion diffusion can be neglected because the ion trajectories are mainly affected by the mechanical forces, which are relatively strong. Therefore, the vectors enclosed in parenthesis will be inserted in (6)

to consider the combined effect of mechanical forces. The flux tracing result for the line-to-ground configuration with example wind speed +1 m/s is shown in Fig. 6.

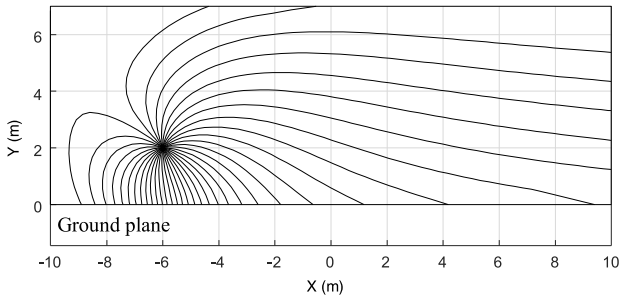

FIGURE 6. Traced flux lines for the unipolar line configuration using the piecewise Bezier curve optimization with example wind speed 1 m/s.

C. CURRENT FLOW MODEL FOR CONTINUITY

Once the electric flux lines are traced, a series of flux tubes can be created by bundling adjacent flux lines. Since the space charges emitted from the conductor surface flow along the flux lines, the ion flow in the flux tube should be conservative.

Applying the Gauss' divergence theorem to the integral form of (3), a current passing through the imaginary surface S_i defined across the flux tube can be defined as

$$I_n = \oint_{S_n} \mathbf{J} \cdot d\mathbf{S}. \tag{14}$$

Combining (2) and (14), the current flows through each surface can be obtained as

$$I_n = \mu \rho_n \mathbf{E} \Delta S_n. \tag{15}$$

Since the currents in the flux tube are conservative, the ion charge density at each node on the flux tube can be expressed in terms of the charge density at the conductor surface as follows.

$$\rho_n = \rho_e \frac{E_{on} \Delta S_0}{E_n \Delta S_n} \tag{16}$$

where ρ_e is the emitting charge density at the conductor surface, and E_{on} is the corona onset gradient of the conductor defined as [24].

Since the space charge always moves along the flux line, the electric field vectors in (15) can be replaced by their magnitudes, and the direction is considered by defining ΔS to be perpendicular to each flux line.

Once the space charge distribution is calculated, the electric field in (6) is updated to trace a new set of flux lines. To evaluate the ion flow field in space, each flux tube is divided into triangle elements, and the values for space charge density are assigned to each node.

The electric field at any point in space can be obtained by integrating the effect of the surface charges on the conductor and the space charges flowing through the flux lines. Based on the Gauss' law,

$$\mathbf{E}(\mathbf{r}) = \frac{1}{2\pi\varepsilon_0} \left[\int_{S'} \frac{\sigma(\mathbf{r}'_i)}{R_i^2} \hat{R}_i ds' + \int_{\Omega'} \frac{\rho(\mathbf{r}'_j)}{R_j^2} \hat{R}_j d\Omega' \right] \tag{17}$$

where $\hat{R}$ represents the direction from the source (primed) to observation (unprimed) coordinates. The charge densities σ and ρ represent the charges on the conducting surface S and space domain Ω, respectively, and they also contain their image charges to consider the ground effect.

The new set of flux lines based on (17) is used to modify the space charge distribution as in (16), and the electric field will be updated by the modified space charge distribution. It will be repeated until the space charge density deviates less than the predefined tolerance δ_C, and a terminate condition is satisfied, which can be expressed in terms of the electric potential at the conductor surface. Based on a relation between the electric field and potential, the terminate condition is defined as

$$U_C = -\int_{\Gamma} \mathbf{E} \cdot dl \tag{18}$$

where U_C is the induced voltage, and Γ is an arbitrary path connecting the point with zero potential to the conductor surface. Once the space charge density converges, the amount of emitting charge on the conductor surface is iteratively modified to satisfy the condition in (18). The entire process for the calculation of ion flow field based on the Bezier curve optimization is described in Fig. 7.

III. NUMERICAL RESULT AND DISCUSSION

A. CONCENTRIC CYLINDER

To verify the proposed algorithm, the numerical result for simple electrode configuration is compared to its analytic solution. The analytic solution for the concentric cylindrical configuration is derived in [1], which can be expressed in one-dimensional form using the axial symmetry. The inner and outer conductor radius values are $r_0 = 0.1$ m and $R = 1$ m, respectively. The coronating surface of the inner conductor was divided into 22 segments, and the flux lines were optimized starting from the inner conductor and terminating at the outer conductor. The resulting ion current density is shown in Fig. 8. Due to the axial symmetry, the electric flux lines were not influenced by the modified space charge distribution, and the calculation process for the space charge density turned into a simple two-point boundary value problem. In Fig. 8, we can see a good agreement between the calculated result and the analytic solution.

B. SINGLE UNIPOLAR LINE CONFIGURATION

The proposed algorithm was applied to a simple conductor-plane configuration. For comparison, the experimental setup in [25] was selected as a reference. A unipolar DC line with a conductor radius $r_0 = 0.0025$ m are located above the ground plane with the height $h = 2$ m. In this case, a still air condition was assumed for simplicity. The magnitude of the corona onset gradient for the given conductor is $E_c = 48.06$ kV/cm, based on Peek's law [24].

The surface of the coronating conductor was divided at an interval of 5 degrees, and 72 flux lines were traced in the

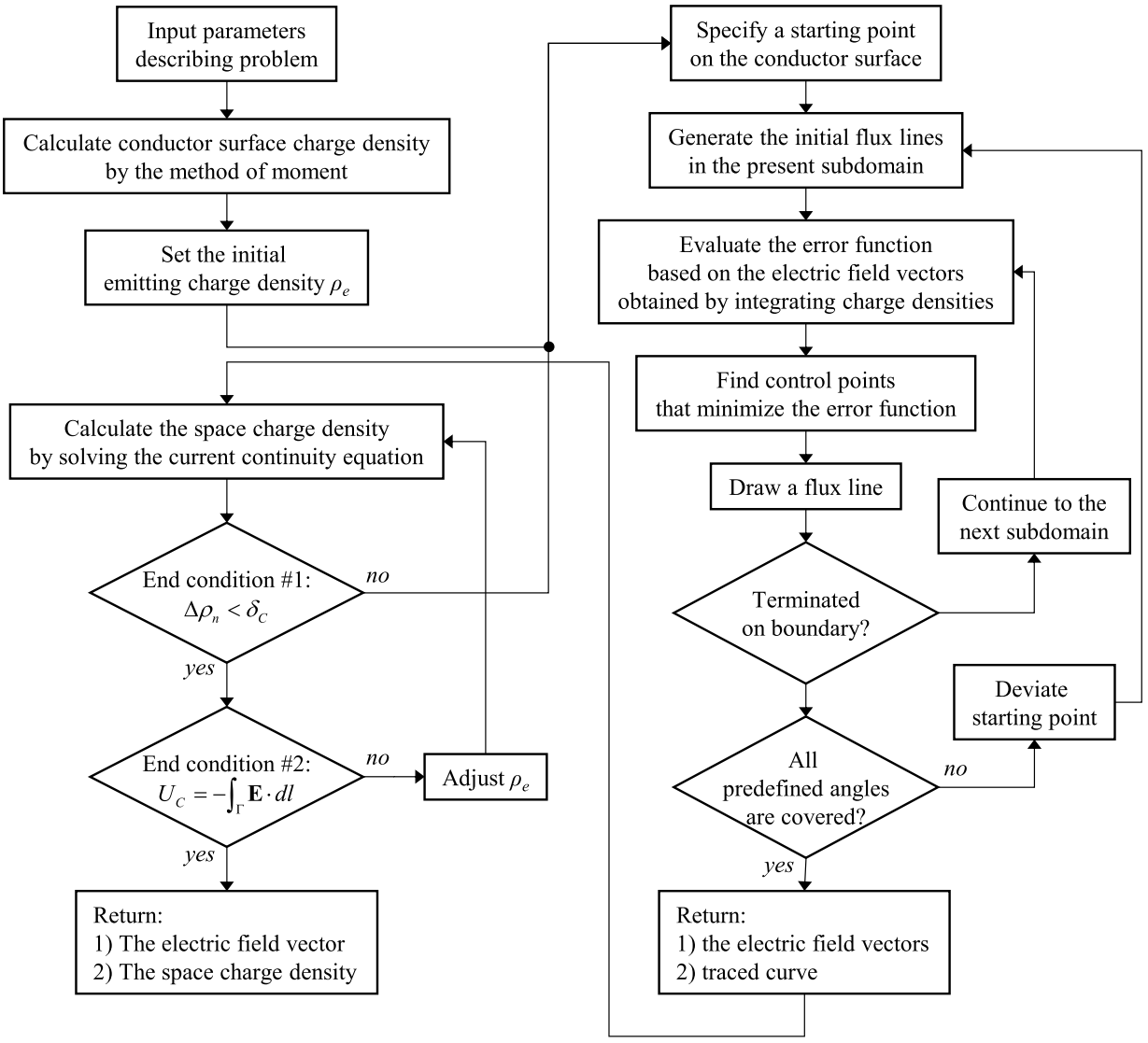

FIGURE 7. Flowchart for the entire process of the ion flow field calculation based on the piecewise Bezier curve optimization.

target domain. For the electric field calculation, the solution domain is divided into 5132 elements with 2640 nodes.

The optimized flux lines for the target configuration is shown in Fig. 9, and Fig. 10 shows the ground profiles of electric field strength with the induced voltage of +200 kV calculated by the proposed method were compared to the experimental result in [25]. The calculated result shows a good agreement with the measured value. However, since the average value of the space charge density was used in each element to evaluate the electric field in (17), the difference in the magnitude appeared as the distance from the conductor increased. The result can be improved by introducing a interpolate functions to the nodal space charge distribution.

C. BIPOLAR HVDC TRANSMISSION LINE

For a one-year period, long-term measurements of ground profiles of the electric field were made by Korea Electric Power Research Institute (KEPRI) for a double bipolar ±500 kV HVDC full-scale test line in Gochang, Korea. The

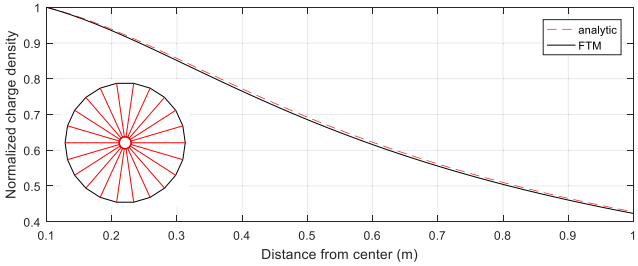

FIGURE 8. Normalized charge density for concentric cylindrical model.

line configuration contains of two bipolar six-bundled lines with metallic return conductors. The heights of the lower and upper conductors are 21 m and 37 m, respectively. Pole spacings of the lower conductors and the upper conductors are 23.8 m and 22.8 m, respectively. Six subconductors are bundled with 30.4 mm diameter and 40 cm bundle spacing. More detailed tower configuration is presented in [26]. In the calculation, the value of conductor surface roughness factor m is assumed to be 0.7.

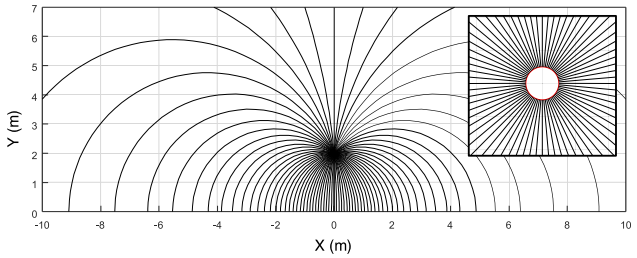

FIGURE 9. Optimized flux lines for the unipolar line configuration.

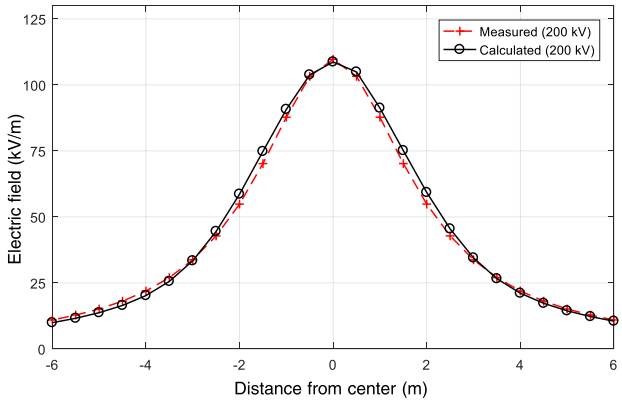

FIGURE 10. Comparison of measured and calculated ground profiles of unipolar ion flow field strength.

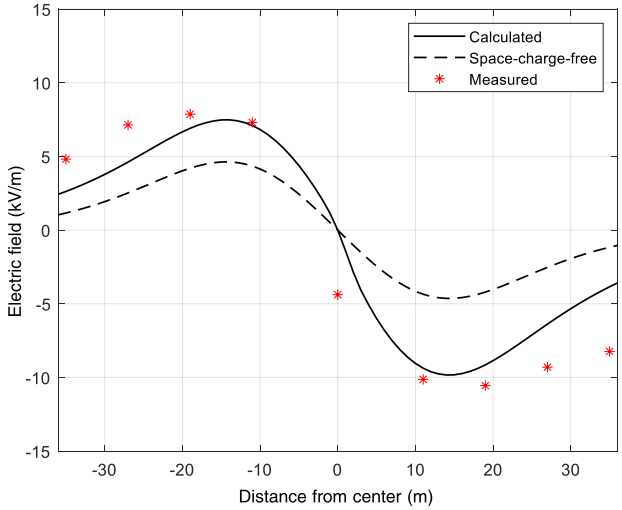

FIGURE 11. Comparison of measured and calculated ground profiles of bipolar ion flow field strength with space-charge-free field.

The calculated ground profile of bipolar ion flow field compared to the measurements is shown in Fig. 11. The difference between the magnitudes of the results is mostly due to weather conditions. Since different seasons and weather conditions are considered in the long-term measurement, the decreased corona onset gradient due to humidity or roughened conductor surface can cause more emission of space charges [9]. Therefore, it should only be meaningful to understand the overall trend of the results.

To verify the effectiveness, the proposed method was compared with the conventional potential-based method while changing the size of analysis domain. Since the long-term measurements contain various uncertainties, it cannot be said

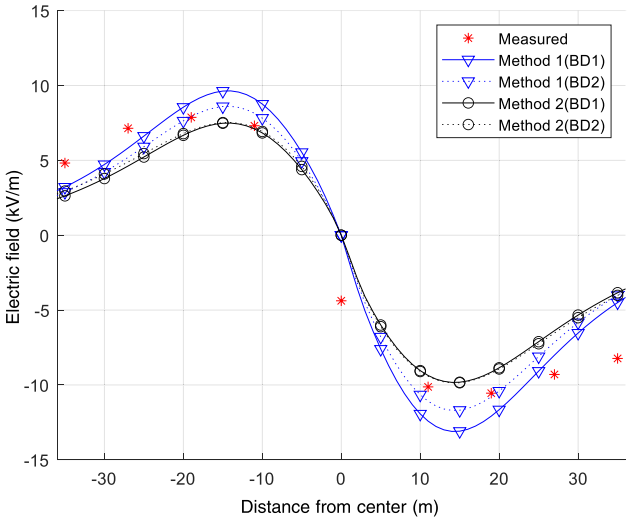

FIGURE 12. Comparison of ground profiles of bipolar ion flow field strength between two methods for expanded boundary; Method 1: potential-based FTM; Method 2: integral-based FTM; BD2: expanded boundary to 150% of BD1.

that the results of numerical analysis are unconditionally accurate just because they are close to the measurements. Therefore, it would be helpful to judge the stability of the analysis method by checking the variation of the calculated result with the change of the domain rather than the exact calculation of the absolute value.

The ground profiles of bipolar ion flow field by two different methods are compared in Fig. 12. The conventional potential-based method is named as Method 1, and the proposed integral-based method is named as Method 2. Both methods are applied to the same calculation domain BD1, and the results are drawn with solid lines. Then, the outmost boundary for BD1 is expanded to 150% and named as BD2. The results are drawn with dotted lines. As shown in Fig. 12, the negative peak value in Method 1 was increased by 10.7% while that of Method 2 increased by 0.375%. This is an error caused by the outermost boundary condition that forces the potential to zero on an artificial boundary that is not far enough. On the other hand, in the case of an integral-based method that does not require the outermost boundary condition, the dependence on the analysis domain is relatively low, and the calculation domain can be minimized without compromising the validity of the results.

IV. CONCLUSION

A new method for tracing the electric flux lines is proposed based on a parametric curve. Defining an error function using the relation between the derivative of the parametric curve and the electric field itself, errors accumulated through the iterations for the numerical differentiation can be minimized.

Once the electric flux lines are traced, a series of flux tubes is created by bundling adjacent flux lines, and the nodal electric field and space charge distribution are iteratively updated. The space charge distribution can be calculated based on the current conservation along the flux tube, and the ion flow field is obtained by integrating the charge densities.

The proposed method was applied to calculate the ion flow field distributions of the concentric cylindrical, a unipolar line-to-ground, and full-scaled test line model. Since the proposed method is based on an integral equation, it is possible to increase the computational efficiency by deriving a closed-form equation or by using a technique such as a Gaussian quadrature. However, singularity problems that occur in the calculation at its own location must be properly considered to increase the accuracy of numerical integration.

To prove the stability of the proposed method, calculations were performed while changing the size of analysis domain, and it was concluded that the dependence on the analysis domain was clearly lower than that of the conventional method.

REFERENCES

[1] P. S. Maruvada, *Corona Performance of High-Voltage Transmission Lines*. Baldock, U.K.: Research Studies Press, 2000, p. 180.
[2] J. S. Townsend, "XI. The potentials required to maintain currents between coaxial cylinders," *London, Edinburgh, Dublin Phil. Mag. J. Sci.*, vol. 28, no. 163, pp. 83–90, Jul. 1914.
[3] W. Deutsch, "Über die dichteverteilung unipolarer ionenströme," *Annalen Physik*, vol. 408, no. 5, pp. 588–612, 1933.
[4] M. P. Sarma and W. Janischewskyj, "Analysis of corona losses on DC transmission lines: I—Unipolar lines," *IEEE Trans. Power App. Syst.*, vol. PAS-88, no. 5, pp. 718–731, May 1969.
[5] M. Sarma and W. Janischewskyj, "Analysis of corona losses on DC transmission lines part II—Bipolar lines," *IEEE Trans. Power App. Syst.*, vol. PAS-88, no. 10, pp. 1476–1491, Oct. 1969.
[6] J. E. Jones and M. Davies, "A critique of the Deutsch assumption," *J. Phys. D, Appl. Phys*, vol. 25, no. 12, pp. 1749–1750, 1992.
[7] V. Amoruso and F. Lattarulo, "Investigation on the Deutsch assumption: Experiment and theory," *IEE Proc. Sci., Meas. Technol.*, vol. 143, no. 5, pp. 334–339, Sep. 1996.
[8] W. Li, B. Zhang, R. Zeng, and J. He, "Discussion on the Deutsch assumption in the calculation of ion-flow field under HVDC bipolar transmission lines," *IEEE Trans. Power Del.*, vol. 25, no. 4, pp. 2759–2767, Oct. 2010.
[9] P. S. Maruvada, "Electric field and ion current environment of HVDC transmission lines: Comparison of calculations and measurements," *IEEE Trans. Power Del.*, vol. 27, no. 1, pp. 401–410, Jan. 2012.
[10] P. S. Maruvada, "Influence of ambient electric field on the corona performance of HVDC transmission lines," *IEEE Trans. Power Del.*, vol. 29, no. 2, pp. 691–698, Apr. 2014.
[11] P. S. Maruvada, "Influence of wind on the electric field and ion current environment of HVDC transmission lines," *IEEE Trans. Power Del.*, vol. 29, no. 6, pp. 2561–2569, Dec. 2014.
[12] B. Zhang, J. Mo, H. Yin, and J. He, "Calculation of ion flow field around HVDC bipolar transmission lines by method of characteristics," *IEEE Trans. Magn.*, vol. 51, no. 3, pp. 1–4, Mar. 2015.
[13] B. Zhang, J. Mo, and J. Liu, "Calculation of ion flow fields of HVDC transmission lines by coupling flux tracing method with finite element method," in *Proc. IEEE Int. Conf. High Voltage Eng. Appl. (ICHVE)*, Sep. 2020, pp. 1–4.
[14] J. Qiao, J. Zou, and B. Li, "Calculation of the ionised field and the corona losses of high-voltage direct current transmission lines using a finite-difference-based flux tracing method," *IET Gener., Transmiss. Distribution*, vol. 9, no. 4, pp. 348–357, Mar. 2015.
[15] J. Qiao, P. Zhang, J. Zhang, Y. Lu, J. Zou, J. Yuan, and S. Huang, "An iterative flux tracing method without Deutsch assumption for ion-flow field of AC/DC hybrid transmission lines," *IEEE Trans. Magn.*, vol. 54, no. 3, pp. 1–4, Mar. 2018.
[16] M. Abdel-Salam and Z. Al-Hamouz, "Finite-element analysis of monopolar ionized fields including ion diffusion," *J. Phys. D, Appl. Phys.*, vol. 26, no. 12, p. 2202, 1993.
[17] M. Abdel-Salam, M. T. El-Mohandes, and S. Kamal El-deen, "A simplified method for quick calculation of corona I–V characteristics of unipolar transmission-line configurations," *IEEE Trans. Plasma Sci.*, vol. 48, no. 3, pp. 631–642, Mar. 2020.
[18] T. Takuma and T. Kawamoto, "A very stable calculation method for ion flow field of HVDC transmission lines," *IEEE Trans. Power Del.*, vol. PWRD-2, no. 1, pp. 189–198, Jan. 1987.
[19] B. L. Qin, J. N. Sheng, Z. Yan, and G. Gela, "Accurate calculation of ion flow field under HVDC bipolar transmission lines," *IEEE Trans. Power Del.*, vol. 3, no. 1, pp. 368–376, Jan. 1988.
[20] X. Li, "Numerical analysis of ionized fields associated with HVDC transmission lines including effect of wind," Ph.D. dissertation, Dept. Elect. Comput. Eng., Univ. Manitoba, Winnipeg, MB, Canada, 1997.
[21] B. Zhang, J. He, R. Zeng, S. Gu, and L. Cao, "Calculation of ion flow field under HVdc bipolar transmission lines by integral equation method," *IEEE Trans. Magn.*, vol. 43, no. 4, pp. 1237–1240, Apr. 2007.
[22] J.-H. Kim, Y.-S. Chung, G. M. Kwon, K. Y. Shin, and H.-K. Jung, "Calculation of ion flow fields of HVdc transmission lines based on error minimization using nodal current density," *IEEE Trans. Magn.*, vol. 55, no. 6, pp. 1–4, Jun. 2019.
[23] N. A. Kapzow, *Elektrische Vorgänge in Gasen und im Vakuum (Hochschulbücher für Physik)*, 2nd ed. Berlin, Germany: Deutscher Verlag der Wissenschaften, 1955, p. 714.
[24] F. W. Peek, *Dielectric Phenomena in High Voltage Engineering*. New York, NY, USA: McGraw-Hill, 1920.
[25] M. Hara, N. Hayashi, K. Shiotsuki, and M. Akazaki, "Influence of wind and conductor potential on distributions of electric field and ion current density at ground level in DC high voltage line to plane geometry," *IEEE Trans. Power App. Syst.*, vol. PAS-101, no. 4, pp. 803–814, Apr. 1982.
[26] K. Y. Shin, J. A. Oh, G. M. Kwon, M. N. Ju, and J. M. Woo, "Long-term evaluation of HVDC transmission line audible noise and its correlation with background noise," *AIP Adv.*, vol. 9, no. 9, Sep. 2019, Art. no. 095014.

JIN-HYEOK KIM was born in Incheon, South Korea, in 1985. He received the B.S. degree in electrical engineering from the State University of New York at Stony Brook, New York, NY, USA, in 2013, and the Ph.D. degree in electrical engineering from Seoul National University, Seoul, South Korea, in 2020.

Since 2021, he has been a Senior Researcher with the Korea Research Institute of Standards and Science, Daejeon, South Korea. His research interests include numerical analysis of high voltage applications, partial discharges, and power system operations.

SUNGJUNG JOO was born in Seoul, South Korea, in 1977. He received the B.S. and Ph.D. degrees in physics from Korea University, Seoul, in 2005 and 2011, respectively.

Since 2020, he has been a Senior Researcher with the Korea Research Institute of Standards and Science, Daejeon, South Korea. His research interests include precision measurement and metrology of electricity and magnetism.

YOUNG-SEEK CHUNG (Member, IEEE) received the B.S., M.S., and Ph.D. degrees in electrical engineering from the Seoul National University, Seoul, South Korea, in 1989, 1991, and 2000, respectively.

From 1991 to 1996, he was with the Living System Laboratory, LG Electronics. From 1998 to 2000, he was a Teaching Assistant of electrical engineering with Seoul National University. From 2001 to 2002, he was with Syracuse University, Syracuse, NY, USA. From 2003 to 2006, he was a Faculty Member of the Department of Communication Engineering, Myongji University, South Korea. Since 2006, he has been a Professor with the Department of Electronic Convergence Engineering, Kwangwoon University, Seoul. His research interests include numerical analysis of inverse scattering problem using time-domain techniques, EMI/EMC for industrial applications, and radar signal processing.